Christoph M. Arndt, Michael J. Papageorge, Frederik Fuest, Jeffrey A. Sutton, Wolfgang Meier

Experimental Investigation of the Auto-Ignition of a Transient Propane Jet-in-Hot-Coflow

Proceedings of the Combustion Institute 37(2) (2019), 2117-2124.

The original publication is available at www.elsevier.com
https://doi.org/10.1016/j.proci.2018.06.195

Experimental Investigation of the Auto-Ignition of a Transient Propane Jet-in-Hot-Coflow

Christoph M. Arndt[a,*], Michael J. Papageorge[b], Frederik Fuest[b,c], Jeffrey A. Sutton[b], Wolfgang Meier[a]

[a] *German Aerospace Center (DLR), Institute of Combustion Technology*
Pfaffenwaldring 38-40, D-70569 Stuttgart, Germany
[b] *The Ohio State University, Department of Mechanical and Aerospace Engineering*
201 West 19th Avenue, Columbus, OH 43210, USA
[c] *Present Address: LaVisison GmbH*
Anna-Vandenhoeck-Ring 19, D-37081 Göttingen, Germany

**Corresponding Author, christoph.arndt@dlr.de*

Abstract

Auto-ignition is a complex process which is extremely sensitive to boundary conditions such as local temperature, mixture or strain rate and occurs on very short time-scales. Therefore, measurement techniques with high spatio-temporal resolution have to be applied to test cases with well-defined boundary conditions in order to generate high-quality validation data for numerical simulations. In the current paper, the auto-ignition of a transient propane jet-in-hot coflow was studied with high-speed OH* chemiluminescence imaging and high-speed Rayleigh scattering for the simultaneous determination of mixture fraction, mixture temperature and scalar dissipation rate immediately prior to the onset of auto-ignition. A variation of the coflow temperature showed a pronounced temperature dependence of the auto-ignition location and time, and the temperature sensitivity was higher than for a comparable methane test case from the literature. This is explained by the lower sensitivity of propane ignition delay times to the local strain rate in comparison to methane. The Rayleigh measurements however showed that the formation mechanism of auto-ignition kernels is similar for propane and methane. Ignition kernels were found to form upstream of bulges of the inflowing jet at locations with locally low scalar dissipation rate.

Keywords

Auto-Ignition; Jet-in-Hot-Coflow; Boundary Conditions; High-Speed Laser Diagnostics; Rayleigh Scattering

1. Introduction

Auto-ignition plays a key role in flame initiation and flame stabilization in internal combustion engines (ICEs) based on diesel or homogeneous compression charge ignition (HCCI) combustion, and in gas turbine (GT) combustors. In contrast, auto-ignition is to be avoided in premixing sections of GT combustors employing reheat combustion, or spark-ignition ICEs, where auto-ignition is known as "engine knock".

Since auto-ignition is a complex process which occurs on short time scales and is very sensitive to thermal, mixing, and flow boundary conditions, experimental studies in technical systems with detailed diagnostics remain challenging. One option to study auto-ignition in a well-controlled environment with technical relevance and well-documented and reproducible boundary conditions are "Jet-in-Hot-Coflow" burners, which gained significant research interest in recent years [1-8]. In this configuration, (cold) fuel is injected into the hot exhaust gas of a lean hydrogen/air-flame, mimicking the mixing process of recirculated combustion products with fresh gas in GT combustors with recirculation. While several previous studies focused on methane or methane/hydrogen mixtures [1-4, 9], only a few studies with heavier fuels such as ethylene [5, 6, 10], n-heptane [8], DME [7, 11], or propane in laminar [12] and turbulent [11, 13] environments exist. Additionally, previous studies have mainly focused on steady-state jet flames [1-5], while only a few studies on the formation mechanism of auto-ignition kernels exist [6, 14-16]. However, detailed data on auto-ignition of heavier fuels is of great importance, especially when studying flame stabilization in re-circulating combustors with varying Wobbe index [17].

Previous numerical and experimental studies have shown that auto-ignition occurs along the iso-line of the most reactive mixture fraction ξ_{mr}, where the kinetic ignition delay time is minimal [18]. In configurations with cold fuel and hot oxidizer, ξ_{mr} is typically very lean due to the high mixture temperatures at low mixture fractions and the high sensitivity of auto-ignition on temperature. Along the iso-line of ξ_{mr}, ignition kernels form at locations with low scalar dissipation rate [18]. The occurrence of auto-ignition at very lean mixture fractions complicates experimental investigations. For example, Papageorge et al. [11] and Arndt et al. [19] employed laser Rayleigh scattering for the simultaneous measurement of mixture fraction and mixture temperature immediately before the onset of auto-ignition in the DLR Jet-in-Hot-Coflow burner (DLR JHC). Due to the low fuel (in that case methane) content at auto-ignition sites and limited signal-to-noise ratio in the hot coflow, resolving the most reactive mixture fraction was not possible.

The current paper focuses on the detailed characterization of auto-ignition dynamics of propane in Jet-in-Hot-Coflows, since such data is sparse in the literature. One goal is to provide detailed data on the influence of the coflow temperature on the auto-ignition process. A special focus is on the influence of strain and scalar dissipation rate on auto-ignition. Comparing the current data with measurements in the same configuration with methane as fuel allows assessing the influence of strain and scalar

dissipation rate on auto-ignition, as the two fuels feature different strain rate sensitivities. Kinetic calculations of the ignition delay time of both fuels were performed to evaluate the different chemical time scales and thus the influence of strain on the auto-ignition of those two fuels. From an experimental standpoint, the study of propane allows higher quality experimental results from laser Rayleigh scattering in comparison to methane, since the ignition temperature is lower, resulting in higher signal-to-noise ratios in the coflow region. Furthermore, propane has a Rayleigh scattering cross section that is approximately six times larger than that of methane [20], allowing the detection of lower mixture fractions.

2. Experimental

Both the DLR Jet-in-Hot-Coflow Burner (DLR JHC) [11, 15, 19, 21] and the Rayleigh measurement setup [11] have been described previously, so only the key parameters are provided here.

2.1 DLR Jet-in-Hot-Coflow Burner

A schematic of the DLR JHC is shown in Figure 1.

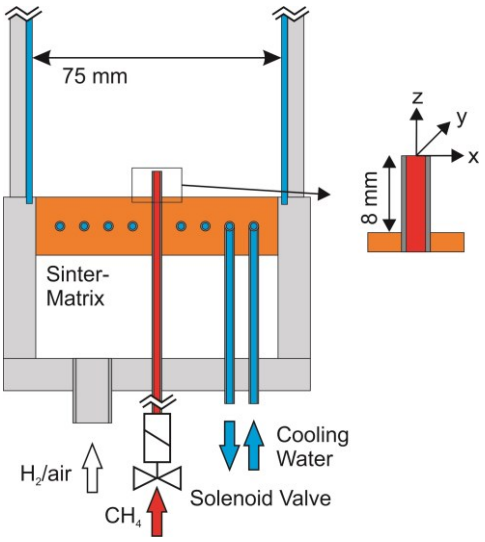

Figure 1. Schematic of the DLR Jet-in-Hot-Coflow Burner.

The hot coflow was generated by a lean premixed hydrogen/air flame stabilized on a quadratic, 75 x 75 mm², water-cooled sintered bronze matrix. Two quartz windows were used to prevent disturbance of the coflow by ambient fluctuations. The laser entrance and exit side windows were removed due to the high laser energies applied. No effect of room air entrainment due to removing the two windows was observed in regions where auto-ignition occurs [19]. The nozzle was a stainless steel tube (inner diameter D = 1.5 mm), the tip of the nozzle was 8 mm above the matrix. Pulses of propane were injected into the hot coflow using a 2/2 way solenoid valve (Staiger VA204-5), located approximately 250 mm (or 165 D) below the nozzle exit to ensure fully developed pipe flow. For the present configuration, the fuel mass flow was 25.7 g/min, the stagnation pressure in front of the solenoid valve was 0.9 bar. A coriolis meter in line with the C_3H_8-injection system was used to calculate the bulk flow velocity (v_{jet} = 134 m/s) and jet exit Reynolds number (Re_{jet} = 39,600).

The coflow operating conditions are summarized in Table 1 along with adiabatic equilibrium temperature (T_{ad}), the measured coflow temperature (T_{cf}), and calculated species mole-fractions based on T_{cf}. The flow rates were controlled with Brooks MFC5850 mass flow controllers and monitored with coriolis flow meters (Siemens Sietrans Mass 2100) with an accuracy of 1.5% [22]. Previous measurements in a similar configuration have shown that the exhaust gas temperature stays very close to T_{ad} if heat loss to the matrix is minimized [23]. To meet this criterion the velocities of the unreacted gas were chosen to exceed 0.7 m/s, the velocity of the hot coflow was v_{cf} = 4.1 m/s for

all operating conditions. The coflow temperature was measured with laser Rayleigh scattering and was approximately 4% below T_{ad} for all examined cases, confirming the minimal heat losses.

	Flow Rates / g/min					Coflow Composition			
φ	Air	H_2	C_3H_8	T_{ad} / K	T_{cf} / K	X_{O_2}	X_{N_2}	X_{H_2O}	ξ_{st}
0.360	343	3.59	25.7	1327	1274	0,1247	0.7264	0.1403	0.0388
0.380	330	3.65	25.7	1374	1319	0.1203	0.7235	0.1475	0.0377
0.400	318	3.70	25.7	1420	1363	0.1160	0.7207	0.1546	0.0365
0.420	311	3.75	25.7	1466	1407	0.1117	0.7180	0.1617	0.0353
0.440	300	3.80	25.7	1510	1450	0.1074	0.7152	0.1688	0.0341
0.460	290	3.85	25.7	1554	1492	0.1032	0.7125	0.1757	0.0329
0.480	278	3.89	25.7	1597	1533	0.0989	0.7097	0.1826	0.0317

Table 1. Operating conditions for the coflow with calculated adiabatic flame temperature T_{ad} (for a fresh gas temperature of 290 K), measured coflow temperature T_{cf} and equilibrium exhaust gas composition [24]. ξ_{st} is the stoichiometric mixture fraction.

Before the measurements, the matrix burner was run for several minutes to achieve thermal equilibrium. Subsequently, a trigger started the laser burst, the recording of the cameras, and the opening of the solenoid valve to start the pulsed jet. This procedure was repeated 30 times at a rate of 0.05 Hz, corresponding to approximately 650 times the coflow advection time (v_{cf} / combustion chamber height). This enabled the flow-field to regain a stationary state without the jet between runs. This sequence was repeated ten times, resulting in 300 individual transient injection/auto-ignition cases.

2.2 Planar Laser Rayleigh Scattering with the High-Energy Pulse-Burst Laser System (HEPBLS) at Ohio State University

Simultaneous mixture fraction and temperature imaging was performed with high-speed planar Rayleigh scattering. To generate the high laser pulse energies necessary for single-shot planar Rayleigh-scattering, the HEPBLS at Ohio State University [25] was used. A continuously operating pulsed Nd:YVO_4 laser was amplified in six flashlamp-pumped Nd:YAG amplifier stages. The first three amplifier stages were operated in a double-pass configuration, the final three amplifier stages were operated in single-pass configuration. Following the last amplification stage, the output beam was frequency doubled to 532 nm. Pulse energies >1 J at 532 nm (pulse duration 25 ns) and burst lengths of 230 pulses were achieved. Since the laser beam had a diameter of approximately 15 mm in the test section, no beam expansion was employed and the laser-sheet was formed by focusing the beam into the test section with a single plano-convex cylindrical lens (f = 750 mm), resulting in a laser-sheet thickness in the test section of <300 µm.

Figure 2 shows the optical and camera setup. A pair of Phantom v711 12-bit high-speed CMOS cameras was used to image the Rayleigh scattering signal from the test section and from a reference air flow for laser-sheet intensity profile and pulse-to-pulse laser energy corrections. Rayleigh scattering from the test section was collected using a combination of a 100 mm-diameter, f = 240 mm achromatic lens and a Nikon, f = 85 mm, f/1.4 camera lens to maximize light collection. The laser-sheet correction camera was outfitted with an 85-mm f/1.4 camera lens.

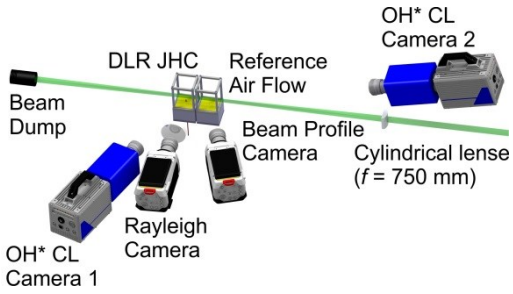

Figure 2. Experimental Setup.

2.3 OH* Chemiluminescence (CL) imaging

Imaging of OH* CL was performed using two intensified 12-bit high-speed CMOS cameras (Photron SA5 with LaVision HS-IRO), equipped with high-throughput UV lenses (Cerco, f = 100 mm, f/2.8, set to f/4.0) and high-transmission bandpass filters (>80 % transmission at 310 nm). One camera, mounted to the left of the Rayleigh cameras, was used to gain information on time and downstream location of the initial auto-ignition event. The second camera was looking along the laser-sheet and was used to determine the position of an ignition kernel relative to the laser-sheet. For the Rayleigh measurements, only ignition kernels that formed within the laser light were evaluated.

2.4 Data Processing

The post-processing and measurement errors of the OH* CL images are discussed in [15, 19, 21] and are not explained here in detail. For the present study the OH* CL images were used for statistical evaluation of the influence of the coflow temperature on ignition time and location and to determine events where the initial auto-ignition occurred within the laser-sheet for the Rayleigh measurements.

Details of the Rayleigh post-processing as well as of the measurement uncertainty can be found in [11, 19]. First, the raw images were darkfield-corrected to account for sensor offset. Non-uniformity in the sensor response was corrected by normalizing each Rayleigh scattering image with an averaged image from ambient air, as described in [25]. Finally, the sheet correction and signal cameras were mapped onto a real-world image size and the spanwise laser-sheet intensity correction was performed using an average of a 25-pixel-wide column from the correction camera. Calculating the mixture fraction and temperature fields from the measured Rayleigh-scattering imaging is a multi-step process, as described in [11]. First the NASA Chemical Equilibrium with Applications (CEA) code [26] is used in conjunction with measured Rayleigh-scattering signals in the coflow to determine the coflow temperature and composition. With the assumption that the equivalence ratio of the coflow is known, a

non-adiabatic temperature (and the associated equilibrium composition) is iterated upon until it converges with that expected from the measured signal ratio of the hot coflow to cold air. After establishing the coflow temperature, an iterative solution procedure is used to determine the local fuel mole-fraction ($X_{C_3H_8}$) and temperature (T) as a function of space and time. For the two-stream mixing problem of cold fuel and the hot oxidizer, the ratio of the local Rayleigh scattering signal S to the Rayleigh scattering signal from cold air at T_{air} = 300 K, is written as

$$S = \frac{X_{C_3H_8} \cdot \sigma_{C_3H_8} + (1 - X_{C_3H_8}) \cdot \sigma_{cf}}{T/T_{air} \cdot \sigma_{air}}, \qquad (1)$$

where $\sigma_{C_3H_8}$, σ_{cf}, and σ_{air} are the Rayleigh cross-sections of propane, coflow, and air, respectively. The relationship between $X_{C_3H_8}$ and T is established by considering enthalpy conservation during mixing of the two streams. Using an enthalpy balance between fuel and coflow along with Eq. 1, a library of signal ratios between Rayleigh-scattering signal (corresponding to $X_{C_3H_8}$ and T) and cold air is calculated. Using the library, the temperature and mole-fraction fields are directly determined from the measured signal ratio. Finally, the data is filtered by a 3x3 pixel median filter to increase the signal-to-noise ratio. The temperature measurement error is <3%, including uncertainties of the mass flow controllers and of the Rayleigh measurement system. Influence of pre-ignition chemistry on the Rayleigh-signal has been evaluated previously [11] and found to be negligible. Furthermore, it was shown in [11] that Rayleigh scattering can be used to measure post-ignition temperatures with an uncertainty of <5% (due to the unknown mixture composition in the measurement volume).

The minimum detectable temperature of a kernel is approximately 3% (or 40 K for T_{cf} = 1275 K) above the coflow temperature. The temporal resolution was 0.1 ms (corresponding to a frame rate of 10 kHz), and the detection of ignition kernels was not limited by spatial resolution. A more sensitive detection of ignition kernels is possible with the simultaneously measured OH* CL.

To accurately resolve mixture fraction gradients, both high SNR and spatial resolution are required. The in-plane spatial resolution was determined using an USAF 1951 target and mixture fraction gradients as high as 4 1/mm could be resolved. The effect of the out-of-plane spatial resolution on the resolvable gradients has not been determined. Measurement noise limits the minimum resolvable spatial gradients, which were 0.04 1/mm in the coflow region ($\xi = 0$); for $\xi > 0$, smaller mixture fraction gradients are resolvable due to higher SNR.

3. Results and Discussions

3.1 Influence of Temperature on Ignition Time and Ignition Height

The dependence of the ignition time τ_{ign} and the ignition height h_{ign} on the coflow temperature T_{cf} is illustrated in Fig. 3.

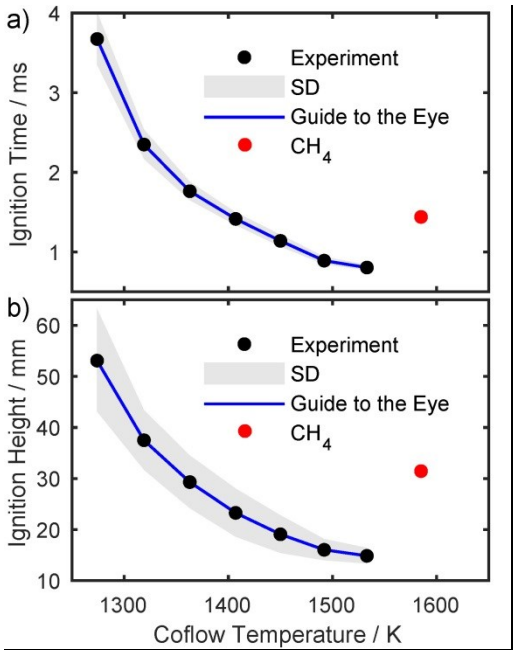

Figure 3. Temperature dependence of a) the ignition time and b) ignition height for propane. The corresponding values for CH_4 (T_{cf} = 1585 K) with matching jet exit velocity are shown in red.

Here, τ_{ign} is defined as the time span between the start of the fuel injection (i.e. the jet exiting the fuel nozzle, confirmed by Rayleigh measurements, similar to [19]) and the occurrence of the first ignition kernel. The ignition height is the axial distance of the centroid of the first ignition kernel (measured with high-speed OH* chemiluminescence) above the fuel nozzle. The symbols correspond to the mean auto-ignition time $\bar{\tau}_{ign}$ (or auto-ignition height $\bar{h}_{ign}$) for each T_{cf}, based on 225 individual ignition events. The grey shaded area corresponds to the standard deviation $\sigma_{\tau_{ign}}$ (or $\sigma_{h_{ign}}$). The blue line serves as a guide to the eye. The mean ignition times were between $\bar{\tau}_{ign}$ = 3.67 ms (with $\sigma_{\tau_{ign}}$ = 0.34 ms or 9.3%) at T_{cf} = 1274 K and $\bar{\tau}_{ign}$ = 0.81 ms (with $\sigma_{\tau_{ign}}$ = 0.04 ms or 4.4%) at T_{cf} = 1533 K. Between 1274 K < T_{cf} < 1319 K, the ignition time has a sensitivity on the coflow temperature of 0.029 ms/K, corresponding to a relative sensitivity of S_{rel} = 12.7. The relative sensitivity is defined as the relative change of a measurement value (in percent) to the relative change of a boundary condition (also in percent):

$$S_{rel} = \frac{\delta\tau_{ign}/\bar{\tau}_{ign}}{\delta T_{cf}/\bar{T}_{cf}}. \qquad (2)$$

This allows a quantitative comparison of the sensitivity of a measurement quantity to different boundary conditions [27]. Between 1492 K < T_{cf} <1533 K, the sensitivity of the ignition time is

0.0021 ms/K or S_{rel} = 3.8. In comparison to the temperature sensitivity of methane in the DLR JHC, propane is more sensitive to a change of T_{cf} (when considering coflow temperatures with similar ignition times) [21, 27]. For example, the sensitivity of methane to the coflow temperature for a mean ignition time of $\bar{\tau}_{ign,CH_4}$ = 3.26 ms is 0.022 ms/K or S_{rel} = 10.2 [27]. However, the measurements with methane were carried out at slightly higher jet exit velocities and lower Reynolds numbers, so the trends for comparable boundary conditions might be different.

Figure 3b) shows the temperature dependence of the ignition height, which is similar to the temperature dependence of the ignition time. With increasing coflow temperature, ignition kernels form closer to the fuel nozzle. For T_{cf} = 1274 K, the mean auto-ignition height was $\bar{h}_{ign}$ = 53.09 mm (with $\sigma_{h_{ign}}$ = 10.09 mm or 19%), for T_{cf} = 1549 K, the ignition height was $\bar{h}_{ign}$ = 14.86 mm (with $\sigma_{h_{ign}}$ = 1.56 mm or 10.5%). In the range 1274 K < T_{cf} < 1319 K, the sensitivity of $\bar{h}_{ign}$ to the coflow temperature was 0.35 mm/K or S_{rel} = 9.2, for 1492 K < T_{cf} < 1533 K, the sensitivity was 0.029 mm/K or S_{rel} = 2.8. The sensitivities are again higher than those of methane for similar ignition heights.

In comparison to measurements with methane [21, 27], both the ignition time and the ignition height for a given temperature are considerably shorter and lower, respectively. For comparable ignition times, the coflow temperature for the methane case was approximately 185 K higher. At T_{cf,CH_4} = 1585 K and the same jet exit velocity as for the current propane case (v_{jet} = 134 m/s), the ignition time for methane was τ_{ign,CH_4} = 1.44 ms. For the C_3H_8-case, the coflow temperature for τ_{ign,C_3H_8} = 1.44 ms was T_{cf,C_3H_8} = 1400 K. The chemical kinetic ignition delay times τ_{id} for the coflow temperatures considered here were calculated using Chemical Workbench [28] and the GRI 3.0 mechanism [29]. They were between 0.07 ms and 1.5 ms for propane, and between 0.2 ms and 1.8 ms for methane (corresponding to a factor between 1.2 and 3 in comparison to propane).

A similar trend is observed for the ignition height. The coflow temperatures for similar ignition heights were approximately 245 K lower for propane (h_{ign,CH_4} = 31.45 mm for T_{cf,CH_4} = 1585 K and v_{jet} = 134 m/s). The coflow temperature for the propane case with the same ignition height is 1340 K. This is considerably lower than the coflow temperature for matching ignition times. One explanation for this behavior is the lower influence of strain on propane auto-ignition, since the ignition chemistry of propane is faster. For methane it was found that the occurrence of locally low strain rates below a critical strain rate is crucial for the onset of auto-ignition [19, 21]. Since the critical strain rate for propane is significantly higher [30], auto-ignition can occur at significantly lower axial positions, where comparably higher strain rate or scalar dissipation rate structures exist.

3.2 Ignition Kernel Formation

The formation of individual ignition kernels was studied with high-speed laser Rayleigh scattering for simultaneously determining mixture fraction, mixture temperature, and scalar dissipation rate immediately prior to the onset of auto-ignition. For the higher coflow temperatures studied here, multiple ignition kernels occur within a short time span. For the case at T_{cf} = 1275 K that is studied in the following section, typically one ignition kernel forms and grows slowly with time until a stable flame is established.

Figure 4 shows the temporal evolution of an exemplary auto-ignition kernel for a coflow temperature of 1275 K.

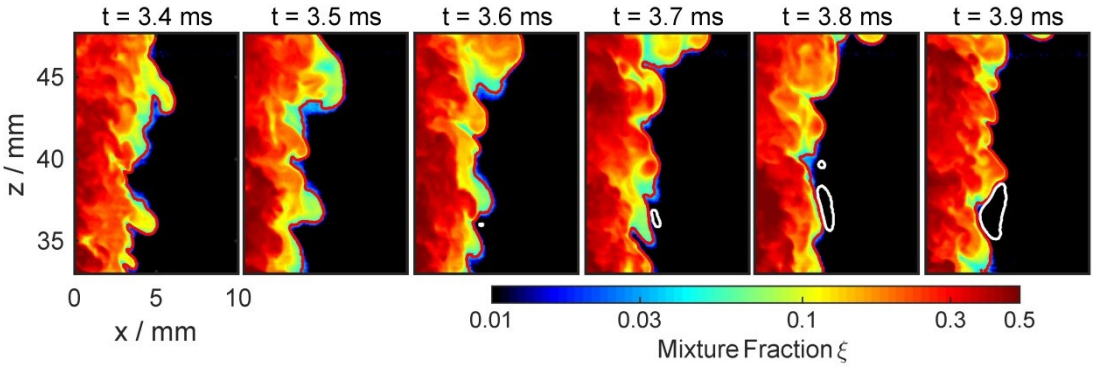

Figure 4. Temporal evolution of the 2D mixture fraction field during an auto-ignition event. Color coded is the mixture fraction with a logarithmic scale, the red iso-line corresponds to the stoichiometric mixture fraction, the white iso-line to T = 1340 K to visualize reacting regions.

For a better overview, only the area to the right of the jet centerline is shown. The mixture fraction is color coded with a logarithmic scale. The red iso-line corresponds to the stoichiometric mixture fraction ξ_{st} = 0.0388, the white iso-line corresponds to a temperature of T = 1340 K and enables the identification of ignition kernels. At t = 3.4 ms, x = 3.5 mm and z = 36 mm, a bulge of the fuel jet is visible. Within this bulge, the mixture fraction is ξ = 0.1. Subsequently, the bulge is transported downstream and its axial extension increases. Simultaneously, the mixture fraction within the bulge decreases to ξ = 0.08 at t = 3.5 ms. Next, the formation of an ignition kernel can be observed upstream of the bulge at x = 4 mm and z = 37 mm, outside of the iso-contour of the stoichiometric mixture fraction. Subsequently, the ignition kernel increases in size, mainly in the axial direction. The minimal resolvable mixture fraction ξ_{min} is approximately 0.005 for the current experiment, (corresponding to 15% of ξ_{st}). The most reactive mixture fraction ξ_{mr} was calculated using Chemical Workbench [28] and the GRI 3.0 mechanism [29] for the coflow temperatures considered here. It was between 3% and 10% of ξ_{st} for propane and on the order of 1% of ξ_{st} for methane.

Figure 5 shows the temperature field for the same auto-ignition event as shown in Fig. 4.

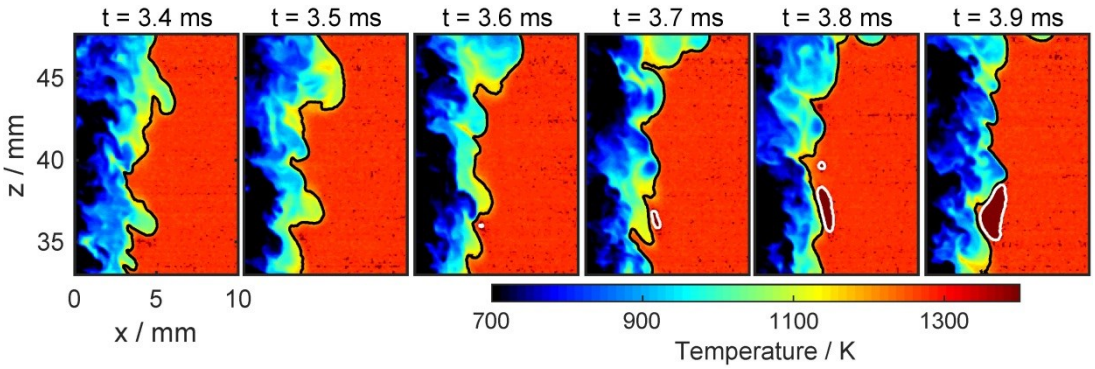

Figure 5. Temporal evolution of the 2D temperature field during the same auto-ignition event as shown in Fig. 4. Color coded is the temperature, the black iso-line corresponds to the stoichiometric mixture fraction and the white iso-line corresponds to T = 1340 K.

The black line corresponds to the iso-line of ξ_{st}, the white iso-line corresponds to T = 1340 K. The bulge where the auto-ignition kernel eventually forms also is visible in the temperature field. Temperatures up to T = 1050 K can be observed within the bulge. At t = 3.6 ms, the ignition kernel forms, and temperatures up to 1600 K occur within the kernel during the image series shown here.

For methane, the strain rate and scalar dissipation rate at the locations where auto-ignition kernels occur play a key role [19, 21]. Therefore, the influence of the scalar dissipation rate on the auto-ignition of propane will be discussed here. In the current measurements, the squared gradient of the mixture fraction $(\nabla\xi)^2$ is used as an approximation for the scalar dissipation rate χ since $\chi = 2D \cdot (\nabla\xi)^2$, where, D is the diffusion coefficient of propane. Figure 6 shows the squared gradient of the mixture fraction for the same auto-ignition event that was discussed in Figs. 4 and 5.

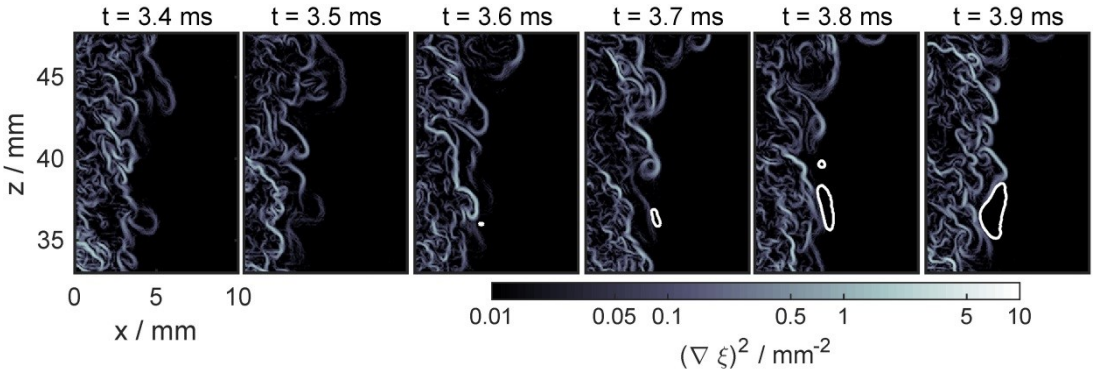

Figure 6. Temporal evolution of the squared gradient of the mixture fraction as a measure of the scaler dissipation rate during the same auto-ignition event shown in Figs. 4 and 5. Note the logarithmic scale. The white iso-line corresponds to T = 1340 K.

The white iso-contour corresponds, as in the previous figures, to T = 1340 K. At t = 3.4 ms and t = 3.5 ms, the bulge at which the auto-ignition kernel eventually forms, is visible as a contour of slightly increased squared mixture fraction gradients on the order of 2 mm^{-2}. During the formation of the ignition kernel at t = 3.6 ms, a slight increase in the local scalar dissipation rate (in comparison to the previous image) can be observed downstream and to the left of the site of the ignition kernel. However, one can assume that the ignition kernel already formed before a distinct increase in

temperature is visible. Therefore, the low scalar dissipation rates at t = 3.5 ms and t = 3.4 ms are much more representative for the formation of the ignition kernel. In the following frames, the scalar dissipation rate drops again, and the ignition kernel slowly grows.

The minimal resolvable mixture fraction was $\xi_{min} \approx 0.005$ (corresponding to 15% of ξ_{st}). In comparison to measurements with methane, where $\xi_{min} \approx 0.015$ (corresponding to 50% of ξ_{st}) [19], the detection limit is significantly improved, predominantly due to the six times larger Rayleigh scattering cross section of propane in comparison to methane [20]. With increased SNR of the current propane experiments (in comparison to methane [19]), it is nearly possible to resolve the very low mixture fractions at the site of auto-ignition kernels, which are approximately 10% of the stoichiometric mixture fraction. Consequently, the influence of strain and scalar dissipation rate on the auto-ignition of different hydrocarbon fuels was assessed based on planar Rayleigh scattering measurements and on chemical kinetic calculations. The measurements have shown that auto-ignition kernels form at the mixture fraction detection limit of the system at mixture fractions $\xi < 0.005$ and at low scalar dissipation rates. Resolving the most reactive mixture fraction, at which ignition kernels form according to numerical simulations [18, 21], was nearly possible with the current data set.

4. Summary and Conclusions

Detailed studies of auto-ignition in a transient propane Jet-in-Hot-Coflow have been performed with optical diagnostics with high spatio-temporal resolution. The auto-ignition location and time were measured with high-speed OH* chemiluminescence imaging and showed a strong dependence on the coflow temperature. The ignition time had a more than 25% higher relative sensitivity to the coflow temperature than the ignition height for all coflow temperatures examined here. This was attributed to the strong dependence of auto-ignition sites on the local scalar dissipation rate, since sites favorable for auto-ignition are less influenced by the coflow temperature than the auto-ignition delay time. The strain rate dependence of propane was found to be lower than in a comparable test case with methane. Since there is a lack of validation data for numerical simulations of auto-ignition in transient jets, especially for heavier hydrocarbons such as propane, the current results contribute to filling this gap.

To further assess the influence of scalar dissipation on the auto-ignition sites, the mixture fraction, mixture temperature and scalar dissipation rate at the site of ignition kernels immediately prior to the onset of auto-ignition were measured with high-speed Rayleigh scattering. In comparison to methane, higher signal-to-noise ratios in the coflow region could be achieved due to the lower coflow temperatures and lower mixture fractions could be resolved due to the higher Rayleigh scattering cross section of propane. It was found that the ignition kernels formed upstream of bulges of the propane jet at locations with locally low scalar dissipation rate, similar to literature results with methane in the same configuration [19].

Future work will focus on the statistical evaluation of the scalar dissipation rate at auto-ignition sites and their influence on the formation and growth of ignition kernels.

References

[1] R. Cabra, T. Myhrvold, J. Y. Chen, R. W. Dibble, A. N. Karpetis, R. S. Barlow, Simultaneous Laser Raman-Rayleigh-LIF Measurements and Numerical Modeling Results of a Lifted Turbulent H2/N2 Jet Flame in a Vitiated Coflow, Proc. Combust. Inst. 29 (2002) 1881-1888.

[2] R. Cabra, J. Y. Chen, R. W. Dibble, A. N. Karpetis, R. S. Barlow, Lifted methane-air jet flames in a vitiated coflow, Combust. Flame 143 (2005) 491-506.

[3] P. R. Medwell, P. A. M. Kalt, B. B. Dally, Simultaneous imaging of OH, formaldehyde, and temperature of turbulent nonpremixed jet flames in a heated and diluted coflow, Combust. Flame 148 (2007) 48-61.

[4] E. Oldenhof, M. J. Tummers, E. H. van Veen, D. J. E. M. Roekaerts, Ignition kernel formation and lift-off behaviour of jet-in-hot-coflow flames, Combust. Flame 157 (2010) 1167-1178.

[5] P. R. Medwell, B. B. Dally, Experimental Observation of Lifted Flames in a Heated and Diluted Coflow, Energy Fuels 26 (2012) 5519-5527.

[6] F. Eitel, J. Pareja, A. Johchi, B. Böhm, D. Geyer, A. Dreizler, Temporal evolution of auto-ignition of ethylene and methane jets propagating into a turbulent hot air co-flow vitiated with NOx, Combust. Flame 177 (2017) 193-206.

[7] A. R. W. Macfarlane, M. J. Dunn, M. Juddoo, A. R. Masri, Stabilisation of turbulent auto-igniting dimethyl ether jet flames issuing into a hot vitiated coflow, Proc. Combust. Inst. 36 (2017) 1661-1668.

[8] J. Ye, P. R. Medwell, M. J. Evans, B. B. Dally, Characteristics of turbulent n-heptane jet flames in a hot and diluted coflow, Combust. Flame 183 (2017) 330-342.

[9] L. D. Arteaga Mendez, M. J. Tummers, E. H. van Veen, D. J. E. M. Roekaerts, Effect of hydrogen addition on the structure of natural-gas jet-in-hot-coflow flames, Proc. Combust. Inst. 35 (2015) 3557-3564.

[10] P. R. Medwell, B. B. Dally, Effect of fuel composition on jet flames in a heated and diluted oxidant stream, Combust. Flame 159 (2012) 3138-3145.

[11] M. J. Papageorge, C. Arndt, F. Fuest, W. Meier, J. A. Sutton, High-speed mixture fraction and temperature imaging of pulsed, turbulent fuel jets auto-igniting in high-temperature, vitiated co-flows, Exp. Fluids 55 (2014) 1763.

[12] B. C. Choi, K. N. Kim, S. H. Chung, Autoignited laminar lifted flames of propane in coflow jets with tribrachial edge and mild combustion, Combust. Flame 156 (2009) 396-404.

[13] Z. Wu, Q. Zhang, L. Li, J. Deng, Z. Hu, R. W. Dibble, Autoignition and Stabilization of Diesel–Propane Lifted Flames Issuing into a Hot Vitiated Co-flow, Energy Fuels 30 (2016) 9730-9736.

[14] W. Meier, I. Boxx, C. Arndt, M. Gamba, N. Clemens, Investigation of Auto-Ignition of a Pulsed Methane Jet in Vitiated Air Using High-Speed Imaging Techniques, J. Eng. Gas Turbines Power 133 (2011) 021504.

[15] C. M. Arndt, J. D. Gounder, W. Meier, M. Aigner, Auto-ignition and flame stabilization of pulsed methane jets in a hot vitiated coflow studied with high-speed laser and imaging techniques, Appl. Phys. B 108 (2012) 407-417.

[16] E. Oldenhof, M. J. Tummers, E. H. van Veen, D. J. E. M. Roekaerts, Transient response of the Delft jet-in-hot coflow flames, Combust. Flame 159 (2012) 697-706.

[17] O. Lammel, M. Severin, H. Ax, R. Lückerath, A. Tomasello, Y. Emmi, B. Noll, M. Aigner, L. Panek High Momentum Jet Flames at Elevated Pressure: A — Experimental and Numerical Investigation for Different Fuels, ASME Turbo Expo 2017: Turbomachinery Technical Conference and Exposition (2017) GT2017-64615.

[18] E. Mastorakos, Ignition of Turbulent Non-Premixed Flames, Prog. Energy Combust. Sci. 35 (2009) 57-97.

[19] C. M. Arndt, M. J. Papageorge, F. Fuest, J. A. Sutton, W. Meier, M. Aigner, The role of temperature, mixture fraction, and scalar dissipation rate on transient methane injection and auto-ignition in a jet in hot coflow burner, Combust. Flame (2016)

[20] J. A. Sutton, J. F. Driscoll, Rayleigh scattering cross sections of combustion species at 266, 355, and 532 nm for thermometry applications, Opt. Lett. 29 (2004) 2620-2622.

[21] C. M. Arndt, R. Schießl, J. D. Gounder, W. Meier, M. Aigner, Flame stabilization and auto-ignition of pulsed methane jets in a hot coflow: Influence of temperature, Proc. Combust. Inst. 34 (2013) 1483-1490.

[22] Siemens, Manufacturer Information (2017).

[23] S. Prucker, W. Meier, W. Stricker, A flat flame burner as calibration source for combustion research: Temperatures and species concentrations of premixed H2/air flames, Rev. Sci. Instrum. 65 (1994) 2908-2911.

[24] C. Morley, Gaseq - A chemical Equilibrium Program for Windows (2005).

[25] M. J. Papageorge, T. A. McManus, F. Fuest, J. A. Sutton, Recent advances in high-speed planar Rayleigh scattering in turbulent jets and flames: increased record lengths, acquisition rates, and image quality, Appl. Phys. B 115 (2014) 197-213.

[26] S. Gordon, B. J. McBride, Computer Program for Calculation of Complex Chemical Equilibrium Compositions and Applications - I. Analysis, NASA Reference Publication 1311 (1994)

[27] C. M. Arndt, Entwicklung und Anwendung von Hochgeschwindigkeits-Lasermesstechnik zur Untersuchung von Selbstzündung, Dissertation, Universität Stuttgart (2017).

[28] Kintech Lab. Chemical Workbench 4.1 (2014)

[29] G. P. Smith, D. M. Golden, M. Frenklach, N. W. Moriarty, B. Eiteneer, M. Goldenberg, C. T. Bowman, R. K. Hanson, S. Song, J. William C. Gardiner, V. V. Lissianski, Z. Qin GRI 3.0. http://www.me.berkeley.edu/gri_mech/

[30] S. Humer, R. Seiser, K. Seshadri, Non-premixed and premixed extinction and autoignition of C_2H_4, C_2H_6, C_3H_6, and C_3H_8, Proc. Combust. Inst. 29 (2002) 1597-1604.